

Cite this: *Org. Biomol. Chem.*, 2012, **10**, 1448

www.rsc.org/obc

PAPER

Kv1.2 potassium channel inhibitors from *Chukrasia tabularis*†

Hong-Bing Liu, Hua Zhang, Ping Li, Yan Wu, Zhao-Bing Gao and Jian-Min Yue*

Received 2nd October 2011, Accepted 14th November 2011

DOI: 10.1039/c1ob06666h

Eighteen new limonoids, chubularisins **A–R** (**1–18**), along with eleven known analogues, were isolated from the stem bark of *Chukrasia tabularis*. The structures of **1–18** were elucidated on the basis of spectroscopic data and chemical evidence. Compound **1** represented the first example of 8,9,12-orthoester of phragmalin limonoids. Interestingly, compounds **4**, **8**, and **22** exhibited potent and selective inhibition against the delayed rectifier (I_K) K^+ current with IC_{50} values of 0.61, 2.03, and 2.15 μ M, respectively.

Introduction

Phragmalin-type limonoids, a class of structurally complex and biologically important compounds attracting a broad range of interests in both organic chemistry and agrochemistry,¹ are the major secondary metabolites of the plants from *Chukrasia* genus (Meliaceae).² Of the two native Southern Chinese species and variety (*Chukrasia tabularis* A. Juss and *Chukrasia. tabularis* var. *velutina*),³ *C. tabularis* has found its applications not only as an economically important timber tree, but also as an astringent, antidiarrheal, and antiinfluenza herb in both traditional Chinese and Indian medicine.⁴ Previous chemical investigations on *C. tabularis* in our research group have led to the isolation of a series of phragmalin-type limonoids from the stem bark, twigs, and leaves (Yunnan province, China)⁵ and from the seeds (Hainan province, China).⁶

Potassium (K^+) channels are implicated in the pathogenesis of severe human diseases, such as long-QT syndromes, atrial fibrillation, epilepsy, Alzheimer's disease, and neuromuscular disorders.⁷ Therefore, they are the attractive targets for rational drug design, and a number of organic modulators of potassium channels have been developed as new drugs or drug candidates.^{7,8}

In our current work, eighteen new phragmalin-type limonoids chubularisins **A–R** (**1–18**), along with eleven known congeners, were isolated from the stem bark of *C. tabularis* collected from Hainan province of China, with some of these compounds exhibiting potent inhibition on the delayed rectifier (I_K) K^+ current. Herein, we describe the separation and structural characterization of these limonoids, as well as the blocking activity of the major isolates on delayed rectifier (I_K) K^+ channel.

Results and discussion

Chubularisin A (**1**) had a molecular formula of $C_{35}H_{42}O_{15}$ based on the HR-ESI(+)MS ion peak at m/z 725.2426 [$M + Na$]⁺ (calcd 725.2416), indicating the presence of fifteen degrees of unsaturation. IR spectrum showed the existence of hydroxyl (3440 cm^{-1}) and carbonyl (1740 cm^{-1}) groups. The ^{13}C NMR spectrum with DEPT (in $CDCl_3$) displayed 35 carbon resonances (Table 1) including eight methyls (including one methoxy), two methylenes, eleven methines (five oxygenated and four olefinic), and fourteen quaternary carbons (four oxygenated and two olefinic). Further analyses of its 1H and ^{13}C NMR (with DEPT) data (Tables 1 and 2) revealed the existence of a methoxyl (δ_H 3.68, s, 3H; δ_C 53.0), an isobutyryl (δ_H 1.19, d, $J = 7.3$ Hz, 3H; 1.21, d, $J = 7.6$ Hz, 3H; and 2.58, (m); δ_C 18.8, 19.3, 33.9, and 175.3), an acetyl (δ_H 2.24, s, 3H; δ_C 21.0 and 170.0), a β -furyl ring (δ_H 6.47, br t, $J = 0.8$ Hz; 7.45, br s, and 7.50, br s; δ_C 110.1, 119.3, 141.7, and 143.5), a typical orthoacetate (δ_H 1.54, s, 3H; δ_C 21.2 and 117.7), and an α,β -unsaturated δ -lactone ring (δ_H 7.12, s and 5.16, s; δ_C 162.1, 117.6, 164.7, 78.5, and 45.5). Three hydroxyl protons at δ_H 2.36 (s), 3.36 (s), and 3.86 (d, $J = 5.1$ Hz) were distinguished from others by HSQC and HMBC spectra. Ten unsaturation degrees were accounted for by four ester carbonyls, one *ortho*-acetate, one olefinic bond, and a β -furyl ring, and the remaining five degrees of unsaturation required **1** to be pentacyclic. The aforementioned data suggested that compound **1** was a phragmalin-type limonoid orthoester.^{2c,5c,6,9,10}

Extensive analysis of 2D NMR data, especially the HMBC spectrum (Fig. 1A), allowed the assignments of most functional groups to the limonoid core and confirmed the framework of **1** as shown. In particular, three hydroxyls were assigned to C-1 (δ_C 81.6), C-2 (δ_C 75.5), and C-3 (δ_C 87.1) by HMBC correlations (1-OH to C-1, C-29, and C-10; 2-OH to C-1, C-2, and C-3; 3-OH to C-2, C-3, and C-4, respectively); the location of the acetoxyl was determined by the HMBC correlation from H-6 (δ_H 5.30, s) to its carbonyl; the isobutyryloxyl was allocated at C-30 (δ_C 66.5) by the HMBC correlation from H-30 (δ_H 5.82, s) to its carbonyl. The methoxyl group was attached to C-7 (δ_C 169.7) as determined

State Key Laboratory of Drug Research, Shanghai Institute of Materia Medica, Chinese Academy of Sciences, 555 Zu Chong Zhi Road, Zhangjiang Hi-Tech Park, Shanghai, 201203, People's Republic of China. E-mail: jmyue@mail.shnc.ac.cn; Fax: +86-21-50806718; Tel: +86-21-50806718

† Electronic supplementary information (ESI) available. See DOI: 10.1039/c1ob06666h

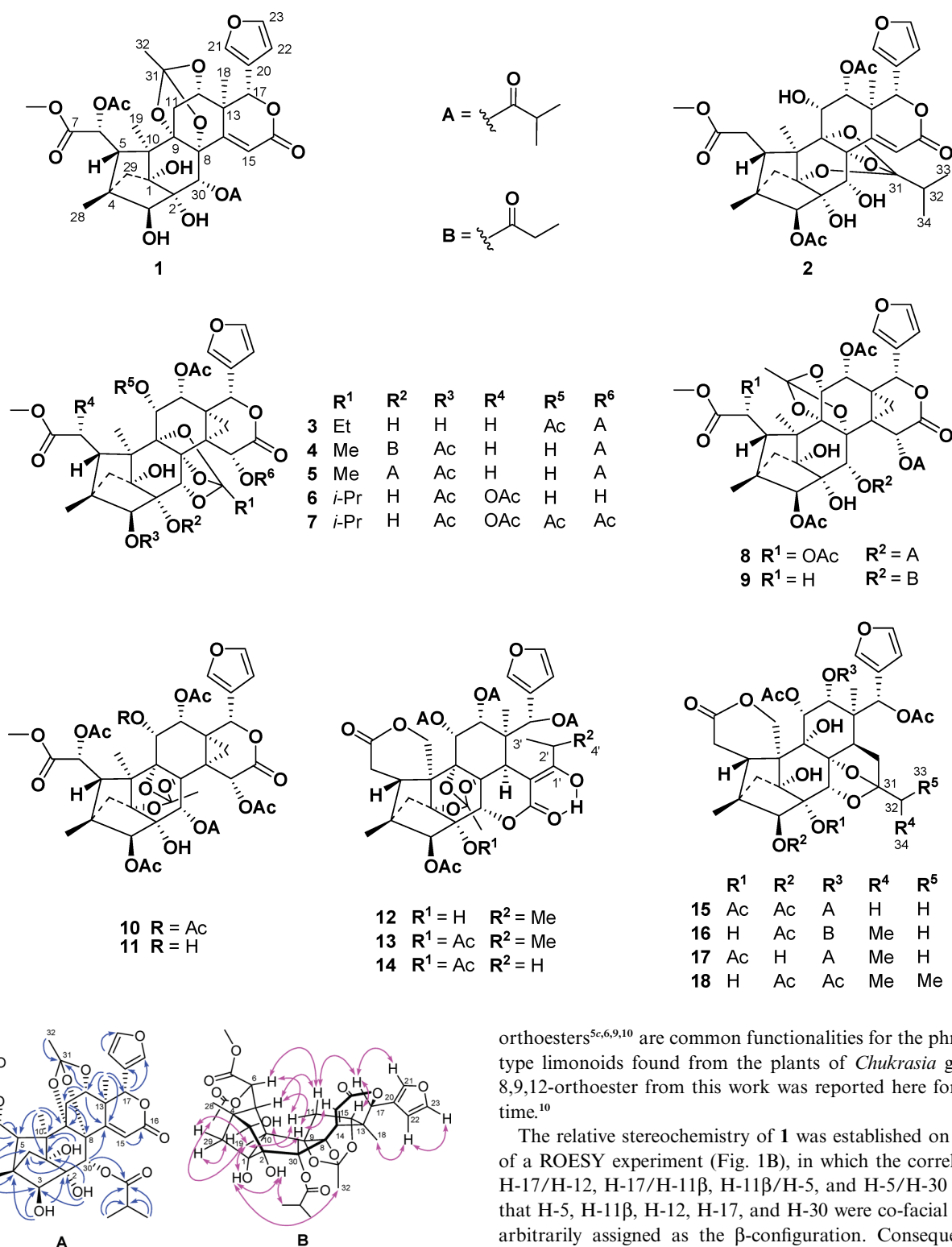


Fig. 1 Selected HMBC (A:→) and ROESY (B:↔) correlations of **1**.

on the basis of HMBC correlation from the OMe to C-7. With the settlement of all the other oxygenated carbons, the 8,9,12-orthoacetate was only attributable to the remaining three oxygenated ones C-8 (δ_C 80.8), C-9 (δ_C 86.0), and C-12 (δ_C 71.7), which was confirmed by one direct HMBC correlation from H-12 (δ_H 3.90, d, J = 4.8 Hz) to C-31. While 1,8,9-,^{2a,2b,5c,9,10} 8,9,11-,^{5c,6,9,10} or 8,9,30-

orthoesters^{5c,6,9,10} are common functionalities for the phragmalin-type limonoids found from the plants of *Chukrasia* genus, the 8,9,12-orthoester from this work was reported here for the first time.¹⁰

The relative stereochemistry of **1** was established on the basis of a ROESY experiment (Fig. 1B), in which the correlations of H-17/H-12, H-17/H-11 β , H-11 β /H-5, and H-5/H-30 indicated that H-5, H-11 β , H-12, H-17, and H-30 were co-facial and were arbitrarily assigned as the β -configuration. Consequently, the ROESY cross-peaks of Me-19/OH-1, Me-19/H-29a, Me-19/H-11 α , H-3/H-29b, 1-OH/2-OH, and Me-32/1-OH revealed that Me-19, Me-32, 1-OH, 2-OH, H-11 α , H-3, and CH₂-29 were α -oriented. The singlet proton H-6 was ascribed to the dihedral angle with H-5 near 90°. In addition, the mutual ROESY cross-peaks of H-6/H-11 α , H-6/H-11 β , and AcO-6/Me-19 confirmed the relative configuration of C-6 to be the same as that in tabularisin A⁶ separated from the same plant and elucidated by single crystal

Table 1 ^{13}C NMR spectroscopic data of **1–11** in CDCl_3 at 100 MHz

No.	1	2	3	4	5	6	7	8	9	10	11
1	81.6	90.6	84.2 ^a	84.4	84.4	84.7	84.4	82.9	82.9	84.3	84.3
2	75.5	76.7	77.0	83.4	83.1	76.4	75.8	76.5	76.4	79.0	78.9
3	87.1	85.3	85.4	85.1	85.1	84.2	85.4	85.9	85.8	83.2	83.3
4	44.0	44.2	44.2	44.6	44.6	45.7	44.2	44.7	44.8	46.5	46.5
5	41.6	39.1	38.1	38.6	38.6	40.7	44.5	42.9	38.0	41.5	41.6
6	72.0	32.3	33.6	33.4	33.4	71.7	71.2	70.6	33.0	71.7	72.1
7	169.7	174.1	174.2	174.0	174.0	170.7	171.9	171.5	173.8	169.3	169.2
8	80.8	77.7	86.9	87.4	87.4	83.4	86.4	78.1	78.3	85.2	85.4
9	86.0	83.6	84.3 ^a	84.6	84.6	83.8	84.1	90.6	90.5	84.9	86.0
10	47.2	43.9	48.2	48.3	48.3	47.0	49.3	45.0	44.0	49.0	48.7
11	28.2	75.9	67.1	67.5	67.5	73.8	66.9	74.7	74.8	65.4	67.6
12	71.7	68.4	66.8	68.4	68.4	69.4	66.5	66.3	66.6	67.1	68.5
13	45.5	42.2	29.3	30.0	30.0	38.6	29.4	30.9	31.1	28.6	28.6
14	162.1	156.6	25.5	25.1	25.1	33.3	25.0	30.7	30.8	27.5	27.9
15	117.6	122.4	70.2	70.1	70.1	72.5	69.5	69.1	69.2	66.4	66.4
16	164.7	164.1	166.4	165.7	165.7	168.2	165.8	166.8	166.9	165.4	165.4
17	78.5	78.8	71.0	72.0	72.0	71.1	71.9	71.3	71.4	72.0	72.2
18	18.1	17.4	15.8	17.1	17.1	19.8	16.1	18.5	18.6	14.9	15.3
19	14.2	13.7	16.9	16.5	16.5	15.6	17.7	15.0	14.6	13.5	13.4
20	119.3	120.7	122.2	122.5	122.5	124.1	122.0	122.1	122.1	123.5	123.4
21	141.7	142.4	141.9	141.9	141.9	140.3	142.0	141.9	142.0	141.4	141.6
22	110.1	110.3	109.8	109.8	109.9	108.0	109.6	109.6	109.7	109.3	109.6
23	143.5	143.0	143.0	143.2	143.2	143.4	143.3	143.3	143.3	143.3	143.4
28	15.6	14.2	14.6	14.3	14.4	15.7	15.4	15.3	14.2	15.9	15.9
29	41.4	39.2	38.9	39.6	39.7	40.5	40.0	39.9	38.9	39.3	39.3
30	66.5	67.7	79.8	76.8	76.8	73.5	79.2	69.8	70.5	71.9	71.9
31	117.7	123.0	117.6	116.4	116.4	122.7	119.3	119.4	119.7	120.5	120.2
32	21.2	29.5	23.1	15.8	15.8	33.4	29.0	16.2	16.2	21.1	21.1
33		17.0	8.0			17.0	16.9				
34		16.9				17.0	16.8				
	30-OA		15-OA	15-OA	15-OA			15-OA	15-OA	30-OA	30-OA
1'	175.3		176.8	174.8	174.8			177.9	177.9	177.9	177.8
2'	33.9		34.2	33.8	33.8			34.0	34.0	34.4	34.4
3'	19.3		19.0	18.8	18.8			19.6	19.7	19.0	19.0
4'	18.8		18.6	18.5	18.5			17.8	17.8	17.8	17.8
				2-OB	2-OA			30-OA	30-OB		
				172.9	175.4			173.3	170.8 ^b		
				28.1	34.3			33.8	27.1		
				9.1	18.8			19.4	9.0		
					18.7			18.7			
7-OCH ₃	53.0	52.3	52.2	52.4	52.4	52.7	53.5	53.6	52.4	53.0	53.0
3-OAc		169.7		168.6	168.6	169.8	169.0	169.1	169.2	169.2	169.2
		21.5		20.9	20.9	20.6	21.0	21.0	21.0	21.0 ^c	21.1
6-OAc	170.0					169.5	168.9	169.1		169.2	169.8
	21.0					21.0	20.7	21.0		21.0 ^c	21.1
11-OAc			169.5				169.2			169.2	
			20.9				21.0			20.7 ^c	
12-OAc		170.9	170.2	170.9	170.9	172.8	170.0	170.6	170.7 ^b	168.9	169.3
		19.9	19.4	19.7	19.7	20.6	19.1	19.6	19.8	19.3	19.8
15-OAc							170.2			169.2	169.4
							21.1			20.6 ^c	20.7

^{a-c}Interchangeable signals within the same column.

X-ray analysis. Therefore, the structure of chubularisin A (**1**) was assigned as shown.

Chubularisin B (**2**) had the molecular formula of $\text{C}_{35}\text{H}_{42}\text{O}_{15}$ as established on the basis of HR-ESI(+)MS ion peak m/z at 725.2415 $[\text{M} + \text{Na}]^+$ (calcd 725.2416). The NMR data (Tables 1 and 2) of **2** were very similar to those of **1**, indicating that compound **2** was also a phragmalin-type limonoid orthoester. The positions of the OH, ester, and orthoester groups were elucidated based on the HMBC data. Three proton signals of hydroxyls at δ_{H} 3.92 (s), 2.79 (s), and 3.07 (s) were distinguished by HSQC data and were assigned to C-2 (δ_{C} 76.7), C-11 (δ_{C} 75.9), and C-30 (δ_{C} 67.7) on observing HMBC correlations (2-OH to C-2, C-3, and

C-30; 11-OH to C-9; 30-OH to C-2, C-8, and C-30, respectively). Two acetoxyls were assignable to C-3 (δ_{C} 85.3) and C-12 (δ_{C} 68.4) based on the observation of HMBC correlations from H-3 and H-12 to their carbonyls. The methoxyl group was attached to C-7 (δ_{C} 174.1) on the basis of HMBC correlation from the OMe (δ_{H} 3.72, s, 3H) to C-7. The remaining oxygenated carbons and the HMBC correlations from Me-33/34 to C-31 (δ_{C} 123.0) and C-32 (δ_{C} 29.5) indicated that **2** was an 1,8,9-*ortho*-isobutyrate. The relative stereochemistry of **2** was assigned based on an explanation of ROESY data (see supporting information S12†). The ROESY correlations of H-12/H-17, H-5/H-12, H-5/H-30, and H-11/H-12 indicated that they are co-facial and arbitrarily assigned as

Table 2 ^1H NMR spectroscopic data of **1–5** in CDCl_3 at 400 MHz

No.	1 (multi., J in Hz)	2 (multi., J in Hz)	3 (multi., J in Hz)	4 (multi., J in Hz)	5 (multi., J in Hz)
3	3.74 (<i>d</i> , 5.1)	5.17 (<i>s</i>)	3.86 (<i>d</i> , 6.0)	5.34 (<i>s</i>)	5.31 (<i>s</i>)
5	2.60 (<i>s</i>)	1.88 (<i>m</i>) ^a	2.61 (<i>m</i>) ^b	2.43 (<i>d</i> , 12.6)	2.43 (<i>d</i> , 12.7)
6	5.30 (<i>s</i>)	a 2.84 (<i>d</i> , 16.5)	a 3.01 (<i>d</i> , 16.9)	a 2.86 (<i>d</i> , 17.1)	a 2.87 (<i>d</i> , 17.0)
		b 2.37 (<i>d</i> , 16.5)	b 2.37 (<i>dd</i> , 16.9, 12.3)	b 2.30 (<i>dd</i> , 17.1, 12.6)	b 2.31 (<i>dd</i> , 17.0, 12.7)
11	α 2.46 (<i>dd</i> , 13.1, 4.8)	4.26 (<i>d</i> , 2.0)	5.62 (<i>d</i> , 4.8)	4.21 (<i>d</i> , 3.8)	4.22 (<i>d</i> , 4.3)
	β 1.76 (<i>d</i> , 13.1)				
12	3.90 (<i>d</i> , 4.8)	4.83 (<i>d</i> , 2.0)	5.30 (<i>d</i> , 4.8)	5.18 (<i>br d</i> , 3.8)	5.19 (<i>br d</i> , 4.3)
15	7.12 (<i>s</i>)	6.41 (<i>s</i>)	7.44 (<i>d</i> , 2.3)	6.97 (<i>br d</i> , 2.4)	6.97 (<i>br d</i> , 2.4)
17	5.16 (<i>s</i>)	5.79 (<i>s</i>)	6.41 (<i>s</i>)	6.42 (<i>s</i>)	6.43 (<i>s</i>)
18	1.40 (<i>s</i> , 3H)	1.76 (<i>s</i> , 3H)	a 2.60 (<i>m</i>) ^b	a 2.93 (<i>dd</i> , 6.2, 2.4)	a 2.94 (<i>dd</i> , 6.5, 2.4)
			b 1.45 (<i>br d</i> , 6.2)	b 1.46 (<i>d</i> , 6.2)	b 1.45 (<i>d</i> , 6.5)
19	1.37 (<i>s</i> , 3H)	1.30 (<i>s</i> , 3H)	1.34 (<i>s</i> , 3H)	1.29 (<i>s</i> , 3H)	1.30 (<i>s</i> , 3H)
21	7.50 (<i>br s</i>)	7.48 (<i>br d</i> , 0.6)	7.49 (<i>br s</i>)	7.53 (<i>br s</i>)	7.54 (<i>br s</i>)
22	6.47 (<i>br t</i> , 0.8)	6.59 (<i>br d</i> , 1.7)	6.30 (<i>br t</i> , 0.9)	6.53 (<i>br d</i> , 1.8)	6.54 (<i>br d</i> , 1.4)
23	7.45 (<i>br s</i>)	7.41 (<i>br t</i> , 1.7)	7.37 (<i>br t</i> , 1.7)	7.39 (<i>br s</i>)	7.40 (<i>br s</i>)
28	1.10 (<i>s</i> , 3H)	0.77 (<i>s</i> , 3H)	0.91 (<i>s</i> , 3H)	0.75 (<i>s</i> , 3H)	0.76 (<i>s</i> , 3H)
29	a 2.12 (<i>d</i> , 10.8)	a 2.24 (<i>d</i> , 12.0)	a 1.79 (<i>d</i> , 11.4)	a 1.97 (<i>d</i> , 11.0)	a 1.98 (<i>d</i> , 10.6)
	b 1.80 (<i>d</i> , 10.8)	b 1.87 (<i>m</i>) ^a	b 1.66 (<i>m</i>) ^c	b 1.68 (<i>d</i> , 11.0)	b 1.67 (<i>d</i> , 10.6)
30	5.82 (<i>s</i>)	4.44 (<i>s</i>)	4.21 (<i>s</i>)	4.93 (<i>s</i>)	4.92 (<i>s</i>)
32	1.54 (<i>s</i> , 3H)	2.30 (<i>m</i>)	1.88 (<i>q</i> , 7.5, 2H)	1.70 (<i>s</i> , 3H)	1.71 (<i>s</i> , 3H)
33		1.12 (<i>d</i> , 6.9, 3H)	1.05 (<i>t</i> , 7.5, 3H)		
34		1.12 (<i>d</i> , 6.9, 3H)			
	30-OA		15-OA	15-OA	15-OA
	2.58 (<i>m</i>)		2.77 (<i>m</i>)	2.71 (<i>m</i>)	2.72 (<i>m</i>)
	1.21 (<i>d</i> , 7.6, 3H)		1.29 (<i>d</i> , 7.0, 3H)	1.19 (<i>d</i> , 7.1, 3H)	1.20 (<i>d</i> , 7.0, 3H)
	1.19 (<i>d</i> , 7.3, 3H)		1.28 (<i>d</i> , 7.0, 3H)	1.24 (<i>d</i> , 6.9, 3H)	1.24 (<i>d</i> , 6.8, 3H)
				2-OA	2-OA
				2.37 (<i>m</i>)	2.62 (<i>m</i>)
				1.13 (<i>t</i> , 7.6, 3H)	1.17 (<i>d</i> , 7.0, 3H)
7-OMe	3.68 (<i>s</i> , 3H)	3.72 (<i>s</i> , 3H)	3.75 (<i>s</i> , 3H)	3.73 (<i>s</i> , 3H)	3.74 (<i>s</i> , 3H)
3-OAc		2.00 (<i>s</i> , 3H)		2.35 (<i>s</i> , 3H)	2.36 (<i>s</i> , 3H)
6-OAc	2.24 (<i>s</i> , 3H)				
11-OAc			2.06 (<i>s</i> , 3H)		
12-OAc		1.62 (<i>s</i> , 3H)	1.52 (<i>s</i> , 3H)	1.63 (<i>s</i> , 3H)	1.64 (<i>s</i> , 3H)
1-OH	2.36 (<i>s</i>)		3.19 (<i>s</i>)	3.52 (<i>s</i>)	3.53 (<i>s</i>)
2-OH	3.36 (<i>s</i>)	3.92 (<i>s</i>)	3.40 (<i>s</i>)		
3-OH	3.86 (<i>d</i> , 5.1)		3.29 (<i>d</i> , 6.0)		
11-OH		2.79 (<i>s</i>)		2.09 (<i>s</i>)	2.10 (<i>s</i>)
30-OH		3.07 (<i>s</i>)			

^{a,b}Overlapping signals within the same column. ^cSignals overlapped by water peak.

β -oriented. ROESY correlations of Me-18/H-22, H-29a/Me-19, H-29b/H-3, Me-19/11-OH, 30-OH/Me-33/34, and 2-OH/H-30 indicated that the furyl ring, Me-18, Me-19, CH_2 -29, 1,8,9-*ortho*-isobutyrate, 2-OH, 11-OH, and 30-OH were α -oriented. The structure of chubularisin B (**2**) was thus characterized as drawn.

Chubularisin C (**3**) was assigned a molecular formula of $\text{C}_{38}\text{H}_{46}\text{O}_{17}$ based on the HR-ESI(+)MS ion peak at m/z 797.2609 $[\text{M} + \text{Na}]^+$ (calcd 797.2627). Analyses of the NMR data (Tables 1 and 2) of **3** implied that it had the same limonoid core as tabularisin C,⁶ and the differences were the positions of the OH, ester, and orthoester groups. Two acetoxys were assignable to C-11 (δ_{C} 67.1) and C-12 (δ_{C} 66.8) on the basis of the HMBC correlations from H-11 (δ_{H} 5.62, *d*, J = 4.8 Hz) and H-12 (δ_{H} 5.30, *d*, J = 4.8 Hz) to their corresponding carbonyls (see supporting information S18†). The HMBC correlations of 1-OH/C-1, C-10, and C-29, 2-OH/C-2 and C-3, and 3-OH/C-2, C-3, and C-4 allowed the assignments of hydroxyls to C-1 (δ_{C} 84.2), C-2 (δ_{C} 77.0), and C-3 (δ_{C} 85.4), respectively. The location of an isobutyryloxyl at C-15 (δ_{C} 70.2) was determined from the HMBC correlation from H-15 to its carbonyl. The *ortho*-propionate was attached to C-8 (δ_{C} 86.9), C-

9 (δ_{C} 84.3), and C-30 (δ_{C} 79.8). The relative configuration of **3** was established by the ROESY data (see supporting information S19†) to be the same as that of tabularisin C⁶ at all the corresponding chiral centers. Thus, the chemical structure of **3** was determined as shown.

Chubularisins D (**4**) and E (**5**) had molecular formulae of $\text{C}_{40}\text{H}_{48}\text{O}_{18}$ and $\text{C}_{41}\text{H}_{50}\text{O}_{18}$, which were acquired from HR-ESI(+)MS data at m/z $[\text{M} + \text{Na}]^+$ 839.2731 (calcd 839.2733, **4**) and 853.2888 (calcd 853.2889, **5**), respectively. The ^1H and ^{13}C NMR data (Tables 1 and 2) of **4** and **5** were highly close to those of tabularisin H,⁹ indicating that they were both phragmalin-type limonoids with an 8,9,30-orthoacetate incorporating a cyclopropanyl ring. By comparison, the only difference between **5** and tabularisin H lay in the reduction of 58 mass units for the former, which suggested a loss of an acetoxy group in **5** that was further confirmed to be at C-6 position by 2D NMR data (see supporting information S32†). Compound **4** is differentiated from **5** merely in the C-2 substitution with the C-2 isobutyryloxyl group in **5** being replaced by a propionyloxyl functionality in **4**, and this alteration was clearly revealed by NMR data (Tables

Table 3 ^1H NMR spectroscopic data of **6–11** in CDCl_3 at 400 MHz

No.	6 (multi., J in Hz)	7 (multi., J in Hz)	8 (multi., J in Hz)	9 (multi., J in Hz)	10 (multi., J in Hz)	11 (multi., J in Hz)
3	4.74 (s)	5.36 (s)	5.48 (s)	5.52 (s)	4.75 (s)	4.75 (s)
5	2.79 (s)	2.80 (s)	2.89 (s)	2.58 (d, 12.6)	3.21 (s)	3.11 (s)
6	5.92 (s)	6.25 (s)	5.91 (s)	a 2.66 (d, 16.6) b 2.45 (dd, 16.6, 2.6)	5.58 (s)	5.29 (s)
11	4.04 (dd, 3.4, 3.1)	5.66 (d, 4.8)	4.23 (d, 3.4)	4.19 (d, 3.1)	5.56 (d, 5.1)	4.17 (br s)
12	5.67 (d, 3.4)	5.42 (d, 4.8)	5.33 (br d, 3.4)	5.15 (br d, 3.1)	5.86 (dd, 5.1, 1.0)	5.73 (br d, 4.2)
15	4.23 (s)	6.93 (s)	7.06 (br d, 2.9)	7.18 (br d, 2.6)	6.08 (d, 2.2)	6.11 (s)
17	4.61 (s)	6.49 (s)	6.44 (s)	6.44 (s)	5.66 (s)	5.68 (s)
18	a 1.66 (d, 6.2) b 1.25 (d, 6.2)	a 2.69 (dd, 7.0, 2.5) b 1.48 (m)	a 2.66 (dd, 7.0, 2.9) b 1.44 (d, 7.0)	a 2.65 (dd, 7.0, 2.6) b 1.45 (d, 7.0)	a 2.52 (dd, 8.2, 2.2) b 1.27 (m)	a 2.74 (br d, 7.6) b 1.26 (m)
19	1.48 (s, 3H)	1.36 (s, 3H)	1.35 (s, 3H)	1.31 (s, 3H)	1.09 (s, 3H)	1.25 (s, 3H)
21	7.49 (br s)	7.49 (br s)	7.49 (br t, 0.8)	7.48 (br s)	7.48 (br s)	7.52 (s)
22	6.30 (br t, 0.9)	6.49 (br d, 1.7)	6.52 (br d, 1.8)	6.51 (br s)	6.44 (br d, 1.7)	6.51 (s)
23	7.37 (br t, 1.7)	7.38 (br t, 1.7)	7.40 (br t, 1.8)	7.40 (br s)	7.39 (br s)	7.42 (s)
28	1.15 (s, 3H)	0.95 (s, 3H)	1.00 (s, 3H)	0.84 (s, 3H)	1.10 (s, 3H)	1.10 (s, 3H)
29	a 2.20 (d, 11.1) b 1.82 (d, 11.1)	a 2.16 (d, 10.8) b 1.83 (d, 10.8)	a 2.16 (d, 11.0) b 1.96 (d, 11.0)	a 1.93 (s, 2H)	a 1.99 (d, 11.1) b 1.77 (d, 11.1)	a 1.98 (d, 11.1) b 1.79 (d, 11.1)
30	5.77 (s)	4.09 (s)	5.37 (s)	5.41 (s)	5.80 (s)	5.76 (s)
32	2.10 (m)	2.14 (m)	1.67 (s, 3H)	1.66 (s, 3H)	1.72 (s, 3H)	1.75 (s, 3H)
33	1.04 (d, 6.8, 3H)	1.05 (d, 6.9, 3H)				
34	1.05 (d, 6.7, 3H)	1.06 (d, 6.9, 3H)				
			15-OA 2.91 (m) 1.32 (d, 7.2, 3H) 1.26 (d, 6.6, 3H) 30-OA 2.52 (m) 1.20 (d, 7.7, 3H) 1.18 (d, 7.2, 3H) 3.80 (s, 3H) 2.21 (s, 3H) ^a 2.23 (s, 3H) ^a	15-OA 2.97 (m) 1.34 (d, 7.3, 3H) 1.27 (d, 6.8, 3H) 30-OB 2.33 (q, 7.5, 2H) 1.14 (t, 7.5, 3H) 3.77 (s, 3H) 2.22 (s, 3H)	30-OA 2.83 (m) 1.22 (d, 6.8, 3H) 1.23 (d, 7.3, 3H) 2.18 (s, 3H) 2.14 (s, 3H) 1.46 (s, 3H) 2.14 (s, 3H)	30-OA 2.83 (m) 1.22 (d, 7.1, 3H) 1.22 (d, 7.1, 3H) 2.18 (s, 3H) 2.13 (s, 3H) 1.61 (s, 3H) 2.13 (s, 3H)
7-OMe	3.76 (s, 3H)	3.79 (s, 3H)			3.79 (s, 3H)	3.77 (s, 3H)
3-OAc	2.07 (s, 3H)	2.05 (s, 3H)			2.06 (s, 3H)	2.03 (s, 3H)
6-OAc	2.14 (s, 3H)	2.20 (s, 3H)			2.18 (s, 3H)	2.18 (s, 3H)
11-OAc		2.21 (s, 3H)				
12-OAc	1.88 (s, 3H)	1.53 (s, 3H)	1.68 (s, 3H)	1.67 (s, 3H)		1.61 (s, 3H)
15-OAc		2.22 (s, 3H)				
1-OH		3.27 (s)	2.86 (s)	2.83 (s)		
2-OH	2.82 (s)	3.48 (s)	3.39 (s)	3.42 (s)	2.83 (s)	2.88 (s)
11-OH	3.92 (d, 3.1)					

^a Interchangeable signals within the same column.

1 and 2). The relative configurations of **4** and **5** remained the same as that of tabularisin H, which was confirmed by ROESY data (see supporting information S26 and S33[†]). The structures of chubularisins D (**4**) and E (**5**) were then characterized.

Chubularisins F (**6**) and G (**7**) displayed pseudo molecular ion peaks $[\text{M} + \text{Na}]^+$ at m/z 799.2434 and 883.2641 in HR-ESI(+)MS, corresponding to molecular formulae of $\text{C}_{37}\text{H}_{44}\text{O}_{18}$ (calcd 799.2420) and $\text{C}_{41}\text{H}_{48}\text{O}_{20}$ (calcd 883.2631), respectively. Comparison of the NMR data of compound **6** (Tables 1 and 3) with those of tabularisin H,⁹ showed that they were structural congeners with the *ortho*-acetate functionality in tabularisin H replaced by an *ortho*-isobutyrate group (δ_{H} 1.04, d, J = 6.8 Hz, 3H; 1.05, d, J = 6.7 Hz, 3H; and 2.10, m; δ_{C} 17.0, 17.0, 33.4, and 122.7) in **6**. Furthermore, the absence of signals belonging to the two isobutyryls in the spectra of **6** indicated these groups were absent, which was also readily inferred from the upfield shifted C-2 ($\Delta\delta_{\text{C}}$ 6.6 ppm) and H-15 ($\Delta\delta_{\text{H}}$ 1.32 ppm) signals. Comparison of ^1H and ^{13}C NMR data (Tables 1 and 3) of **7** with those of **6** suggested that compound **7** was also a phragmalin-type limonoid bearing an 8,9,30-*ortho*-isobutyrate. The only structural difference between them existed in the presence of two additional acetoxyl groups at C-11 (δ_{C} 66.9) and C-15 (δ_{C} 69.5) in **7** replacing the 11-OH and

15-OH in **6**, which was further confirmed by the downfield shifted H-11 ($\Delta\delta_{\text{H}}$ 1.62 ppm) and H-15 ($\Delta\delta_{\text{H}}$ 2.70 ppm) signals of **7** owing to the acetylation effect. The relative configurations of **6** and **7** were assigned the same as that of tabularisin H based on the explanation of ROESY NMR analysis (see supporting information S40 and S47[†]).

Chubularisins H (**8**) and I (**9**) had molecular formulae of $\text{C}_{43}\text{H}_{52}\text{O}_{20}$ and $\text{C}_{40}\text{H}_{48}\text{O}_{18}$, as deduced from the HR-ESI(+)MS data at m/z $[\text{M} + \text{Na}]^+$ 911.2960 (calcd 911.2944) and 839.2753 (calcd 839.2733), respectively. Analysis of the NMR data of **8** (Tables 1 and 3) showed that it was an analogue of tabularisin A.⁶ The only difference between them was an isobutyryloxyl group at C-15 (δ_{C} 69.1) in **8** replacing the acetoxyl at C-15 in tabularisin A, which was supported by the HMBC correlation from H-15 (δ_{H} 7.06, br d, J = 2.9 Hz) to the carbonyl (δ_{C} 177.9) of the isobutyryloxyl. The relative configurations of stereo centers of **8** were assigned to be identical with those of tabularisin A by ROESY spectrum (see supporting information S54[†]). Comparison of NMR data (Tables 1 and 3) for **9** with those for **8** suggested that compound **9** was also a phragmalin-type limonoid bearing an 8,9,11-*ortho*-acetate, with the structural differences being the absence of an acetoxyl group at the C-6 of **9** and a propionyloxyl replacing the isobutyryloxyl

Table 4 ^1H and ^{13}C NMR spectroscopic data of **12–14** in CDCl_3 ^a

No.	12		13		14	
	δ_{H} (multi., J in Hz)	δ_{C}	δ_{H} (multi., J in Hz)	δ_{C}	δ_{H} (multi., J in Hz)	δ_{C}
1		84.8		84.8		84.8
2		76.8		82.8		82.8
3	4.91 (s)	83.9	5.50 (s)	80.9	5.51 (s)	80.8
4		45.8		46.7		46.7
5	2.71 (m) ^b	35.4	2.66 (m) ^c	34.5	2.65 (m) ^d	34.5
6	a 2.69 (m) ^b b 3.08 (dd, 18.7, 5.8)	30.8	a 2.67 (m) ^c b 3.04 (dd, 18.2, 5.5)	30.8	a 2.66 (m) ^d b 3.04 (dd, 17.8, 5.1)	30.8
7		171.9		171.8		171.8
8		79.7		79.2		79.1
9		82.8		82.4		82.4
10		44.9		45.5		45.5
11	5.47 (d, 2.0)	68.6	5.45 (d, 2.3)	68.7	5.46 (d, 2.1)	68.6
12	4.76 (d, 2.0)	69.2	4.79 (d, 2.3)	69.2	4.78 (d, 2.1)	69.2
13		44.8		44.7		45.0
14	3.28 (s)	43.4	3.29 (s)	43.6	3.23 (s)	44.1
15		90.5		90.6		91.8
16		169.8		169.8		169.5
17	5.77 (s)	69.4	5.84 (s)	69.2	5.83 (s)	69.2
18	1.59 (s, 3H)	17.6	1.60 (s, 3H)	17.7	1.60 (s, 3H)	17.9
19	a 4.93 (d, 14.6) b 4.69 (d, 14.6)	67.8	a 4.74 (d, 14.4) b 4.68 (d, 14.4)	67.8	a 4.73 (d, 13.9) b 4.68 (d, 13.9)	67.8
20		122.1		122.0		122.1
21	7.33 (br s)	140.4	7.34 (br s)	140.5	7.34 (br s)	140.5
22	6.28 (br s)	109.8	6.28 (br t, 1.0)	109.8	6.28 (br s)	109.8
23	7.31 (br s)	143.1	7.31 (br t, 1.6)	143.1	7.31 (br s)	143.1
28	1.12 (s, 3H)	14.1	1.11 (s, 3H)	14.3	1.11 (s, 3H)	14.3
29	a 1.91 (d, 11.4) b 2.40 (d, 11.4)	38.8	a 1.85 (d, 11.5) b 2.45 (d, 11.5)	39.2	a 1.85 (d, 11.6) b 2.45 (d, 11.6)	39.2
30	5.06 (s)	73.3	5.41 (s)	73.3	5.41 (s)	73.4
31		119.7		119.5		119.6
32	1.61 (s, 3H)	20.6	1.60 (s, 3H)	20.6	1.60 (s, 3H)	20.6
1'		183.2		183.3		183.3
2'	2.98 (m)	30.3	3.00 (m)	30.3	a 2.58 (m) b 2.40 (m)	25.6
3'	1.12 (d, 7.1, 3H)	20.3	1.16 (d, 6.9, 3H)	20.2	1.24 (t, 6.9, 3H)	11.1
4'	1.30 (d, 6.6, 3H)	18.5	1.31 (d, 6.6, 3H)	18.4		
2-OAc				169.4		169.4
			2.34 (s, 3H)	21.2	2.34 (s, 3H)	21.2
3-OAc		169.8		169.5		169.5
	2.33 (s, 3H)	20.9	2.11 (s, 3H)	21.7	2.10 (s, 3H)	21.7
11-OA		175.0		175.1		175.1
	2.65 (m)	34.1	2.66 (m)	34.1	2.65 (m)	33.9
	1.24 (d, 7.1, 3H)	19.3	1.24 (d, 7.1, 3H)	19.3	1.24 (d, 7.1, 3H)	19.3
	1.20 (d, 6.8, 3H)	18.9	1.20 (d, 6.9, 3H)	18.5	1.21 (d, 7.1, 3H)	18.6
12-OA		175.3		175.3		175.3
	2.12 (m)	33.3	2.12 (m)	33.3	2.13 (m)	33.3
	0.94 (d, 7.1, 3H)	18.9	0.94 (d, 7.1, 3H)	18.9	0.94 (d, 7.2, 3H)	18.9
	0.91 (d, 6.8, 3H)	18.0	0.91 (d, 7.0, 3H)	17.7	0.91 (d, 6.8, 3H)	17.6
17-OA		174.5		174.5		174.3
	2.41 (m)	33.9	2.38 (m)	33.9	2.40 (m)	33.9
	1.07 (d, 7.1, 3H)	18.9	1.06 (d, 7.1, 3H)	18.9	1.06 (d, 6.8, 3H)	18.9
	1.07 (d, 7.1, 3H)	18.3	1.05 (d, 6.8, 3H)	18.1	1.06 (d, 6.8, 3H)	18.1
2-OH	2.92 (s)					
1'-OH	13.58 (s)		13.73 (s)			

^a Data were recorded at 400 MHz (^1H) and 100 MHz (^{13}C). ^{b–d} Overlapping signals within the same column.

at C-30 of **8**. The former structural change obviously caused an upfield shift of C-6 to δ 33.0 in the ^{13}C NMR spectrum of **9**. The relative configuration of **9** was also assumed to be the same as that of tabularisin A⁶ based on the explanation of its ROESY (see supporting information S61†) data.

Chubularisin J (**10**) showed a pseudo molecular ion peak at m/z $[\text{M} + \text{Na}]^+$ 925.2742 (calcd 925.2737) in the HR-ESI(+)MS, consistent with a molecular formula of $\text{C}_{43}\text{H}_{50}\text{O}_{21}$. The NMR

data (Tables 1 and 3) of **10** revealed that it was an analogue of tabularisin C.⁶ With the aid of 2D NMR experiments, the ^1H and ^{13}C NMR signals of **10** were assigned as shown in Tables 1 and 3. The assignments of five acetoxys to C-3 (δ_{C} 83.2), C-6 (δ_{C} 71.7), C-11 (δ_{C} 65.4), C-12 (δ_{C} 67.1), and C-15 (δ_{C} 66.4) were accomplished by the HMBC correlations from H-3 (δ_{H} 4.75, s), H-6 (δ_{C} 5.58, s), H-11 (δ_{H} 5.56, d, J = 5.1 Hz), H-12 (δ_{H} 5.86, dd, J = 5.1, 1.0 Hz), and H-15 (δ_{H} 6.08, d,

Table 5 ^1H and ^{13}C NMR spectroscopic data of **15–18** in CDCl_3 ^a

No.	15		16		17		18	
	δ_{H} (multi., J in Hz)	δ_{C}	δ_{H} (multi., J in Hz)	δ_{C}	δ_{H} (multi., J in Hz)	δ_{C}	δ_{H} (multi., J in Hz)	δ_{C}
1		85.5		86.0		85.3		86.0
2		81.1		73.3		81.8		73.4
3	5.35 (s)	82.9	5.28 (s)	85.3	3.92 (d, 5.4)	84.7	5.26 (s)	85.4
4		45.6		44.7		45.1		44.7
5	2.09 (m) ^b	40.4	2.11 (m) ^d	41.0	2.29 (m) ^f	39.1	2.10 (m) ⁱ	41.0
6	2.30 (m, 2H)	31.3	2.31 (m, 2H) ^e	31.4	2.32 (m, 2H) ^f	31.5	2.31 (m, 2H)	31.4
7		172.5		172.8		173.0		172.9
8		89.6		89.7		89.1		89.7
9		75.2		75.2		75.1		75.2
10		52.3		52.2		52.5		52.2
11	5.64 (d, 3.5)	71.3	5.62 (d, 3.5)	71.3	5.78 (d, 3.6)	71.4	5.59 (d, 3.4)	71.3
12	5.52 (d, 3.5)	71.7	5.51 (d, 3.5)	71.8	5.35 (d, 3.6)	71.8	5.45 (d, 3.4)	72.0
13		41.5		41.5		41.3		41.5
14	3.29 (dd, 11.9, 7.5)	44.4	3.24 (dd, 11.9, 7.9)	43.8	3.19 (dd, 11.9, 7.5)	44.1	3.19 (dd, 11.9, 7.9)	43.6
15	α 2.56 (m) ^c	35.3	α 2.53 (dd, 11.8, 7.9)	33.3	α 2.41 (m)	34.3	α 2.50 (dd, 12.1, 7.9)	31.1
	β 1.97 (m)		β 1.96 (dd, 11.9, 11.8)		β 1.96 (m) ^g		β 1.95 (m) ⁱ	
17	6.08 (s)	71.2	6.17 (s)	71.0	6.24 (s)	71.0	6.16 (s)	71.0
18	0.90 (s, 3H)	19.1	0.92 (s, 3H)	18.7	0.96 (s, 3H)	18.5	0.93 (s, 3H)	18.7
19a	5.01 (d, 13.1)	69.3	5.00 (d, 12.4)	69.4	5.01 (d, 12.6)	69.3	5.00 (d, 12.5)	69.4
19b	4.18 (d, 13.1)		4.18 (d, 12.4)		4.16 (d, 12.6)		4.16 (d, 12.5)	
20		122.4		122.1		121.6		122.1
21	7.48 (s)	140.2	7.50 (br s)	140.4	7.59 (br s)	141.6	7.49 (br s)	140.4
22	6.41 (s)	109.5	6.44 (br s)	109.5	6.42 (br d, 1.0)	109.8	6.42 (br d, 0.9)	109.5
23	7.39 (s)	143.3	7.40 (br s)	143.4	7.36 (br t, 1.7)	143.1	7.38 (br t, 1.6)	143.4
28	0.90 (s, 3H)	15.0	0.92 (s, 3H)	15.0	1.01 (s, 3H)	15.1	0.91 (s, 3H)	15.0
29	a 2.06 (d, 11.1)	38.8	a 2.09 (d, 11.2)	38.3	a 2.05 (m) ^h	38.7	a 2.07 (m) ^j	38.3
	b 2.01 (d, 11.1)		b 1.97 (d, 11.2)		b 1.87 (m)		b 1.96 (m) ^j	
30	4.64 (s)	71.1	4.19 (s)	71.7	4.56 (s)	70.2	4.18 (s)	71.5
31		111.0		113.6		112.8		115.8
32	1.66 (s, 3H)	18.7	2.04 (m, 2H)	26.1	1.99 (m, 2H) ^g	25.8	2.24 (m)	31.5
33			1.10 (t, 7.5, 3H)	8.2	1.06 (t, 7.5, 3H)	7.6	1.10 (d, 7.0, 3H)	17.7
34							1.09 (d, 6.8, 3H)	17.0
	12-OA		12-OB		12-OA			
		175.9		173.4		175.9		
	2.56 (m) ^c	34.0	2.35 (m, 2H) ^e	27.2	2.54 (m)	34.0		
	1.17 (d, 6.8, 3H)	19.0	1.11 (t, 7.5, 3H)	9.0	1.14 (d, 7.0, 3H)	19.0		
	1.15 (d, 6.9, 3H)	18.8			1.12 (d, 7.0, 3H)	18.8		
2-OAc		169.6				170.8		
	2.09 (s, 3H)	20.8			2.11 (s, 3H)	20.8 ^b		
3-OAc		169.1		169.6				169.6
	2.48 (s, 3H)	20.9	2.41 (s, 3H)	21.1			2.40 (s, 3H)	21.1
11-OAc		170.8		170.9		170.0		171.0
	2.09 (s, 3H) ^b	20.8	2.11 (s, 3H) ^d	20.8	2.04 (s, 3H) ^b	20.8	2.12 (s, 3H) ^j	20.9
12-OAc								170.0
							2.06 (s, 3H) ^j	20.6
17-OAc		168.8		169.0		170.5		169.0
	2.09 (s, 3H) ^b	20.5	2.13 (s, 3H)	20.8	2.10 (s, 3H)	21.0 ^b	2.11 (s, 3H) ^j	20.7
1-OH	4.87 (s)		4.48 (s)		4.49 (s)		4.47 (s)	
2-OH			3.66 (s)				3.66 (s)	
3-OH					3.76 (d, 5.4)			
9-OH	3.34 (s)		3.33 (s)		3.23 (s)		3.29 (s)	

^a Data were recorded at 400 MHz (^1H) and 100 MHz (^{13}C). ^{b–j} Overlapping signals within the same column.

$J = 2.2$ Hz) to the corresponding carbonyls of five acetoxyl groups. The attachment of an isobutyryloxyl at C-30 (δ_{C} 71.9) was revealed by the HMBC correlation from H-30 (δ_{H} 5.80, s) to its carbonyl carbon. One proton resonance assignable to OH group displayed HMBC correlations with C-2 (δ_{C} 79.0) and C-3, indicating OH groups at C-2. The remaining oxygenated carbons C-1 (δ_{C} 84.3), C-8 (δ_{C} 85.2), and C-9 (δ_{C} 84.9) indicated compound **10** was an 1,8,9-*ortho*-acetate. The ROESY cross-peaks (see supporting information S68†) of H-5/H-11, H-5/H-12, H-5/H-30, H-17/H-30, H-17/H-5, and H-15/H-30 indicated that H-5, H-11, H-12,

H-17, H-15, and H-30 were co-facial and randomly assigned as β -oriented. The ROESY correlation between H-18b/H-22, Me-19/H-29a, and H-3/H-29b suggested that Me-19, CH_2 -29, the cyclopropyl group and the furyl ring were α -oriented. On the basis of its structure homology with tabularisin C and chemical shifts, the configuration of H-6 was β -oriented and OH-2 was α -oriented. Thus, the structure of chubularisin **J** (**10**) was elucidated.

Chubularisin **K** (**11**) was given a molecular formula of $\text{C}_{41}\text{H}_{48}\text{O}_{20}$ by HR-ESI(+)-MS data at m/z 883.2640 [$\text{M} + \text{Na}$]⁺ (calcd 883.2631). The ^1H and ^{13}C NMR data of **11** (Tables 1 and 3)

were of high similarity to those of **10**, except for the absence of an acetyl group at C-11 in **11**. The chemical shift of H-11 (δ_{H} 4.17, br s) in **11** was upfield shifted $\Delta\delta$ 1.39 ppm compared with that of **10** indicating the lack of 11-Ac. Therefore, compound **11** was assigned to be the 11-deacetyl derivative of **10**.

Chubularisin L (**12**) was assigned a molecular formula of $\text{C}_{46}\text{H}_{38}\text{O}_{18}$ as determined by HR-ESI(+)MS displaying an m/z ion at 921.3516 $[\text{M} + \text{Na}]^+$ (calcd 921.3515). The NMR data (Table 4) of **12** resembled those reported for chukvelutillide F,¹¹ except for the presence of one more acetyl group (δ_{H} 2.33 s, 3H; δ_{C} 20.9 and 169.8) at C-3 (δ_{C} 83.9), which was confirmed by a HMBC correlation (see supporting information S80†) from the H-3 (δ_{H} 4.91) to the corresponding carbonyl. The significant ROESY correlations (see supporting information S81†) of H-12/H-17, H-17/H-30, H-30/H-5, and Me-18/H-14, as well as the ^1H and ^{13}C chemical shifts and coupling patterns, suggested that **12** possessed the same relative configuration as chukvelutillide F. Therefore, the structure of chubularisin L (**12**) was assigned as 3-*O*-acetylchukvelutillide F.

Chubularisins M (**13**) and N (**14**) were found to possess molecular formulae of $\text{C}_{48}\text{H}_{60}\text{O}_{19}$ and $\text{C}_{47}\text{H}_{58}\text{O}_{19}$, as established from HR-ESI(+)MS at m/z $[\text{M} + \text{Na}]^+$ 963.3641 (calcd 963.3621) and 949.3466 (calcd 949.3465), respectively. The ^1H and ^{13}C NMR data of **13** (Table 4) were almost superimposable with those of **12** with just one more acetyl group resolved (δ_{H} 2.34 s, 3H, δ_{C} 21.2 and 169.4), and the downfield shifted C-2 signal (δ_{C} 82.8) of **13** ($\Delta\delta_{\text{C}}$ 6.0 ppm) compared with that of **12** indicated the location of this extra acetyl at C-2 position. The NMR data (Table 4) of compound **14** were closely related with those of **13**, with only replacement of the isopropyl group (δ_{H} 1.16, d, $J = 6.9$, 3H; 1.31, d, $J = 6.6$, 3H; and 3.00, m; δ_{C} 18.4, 20.2, 30.3, and 183.3) at C-1' in **13** by an ethyl group (δ_{H} 1.24, t, $J = 6.9$, 3H; 2.40, m; and 2.58, m; δ_{C} 11.1, 25.6, and 183.3) in **14**. The relative configurations of **13** and **14** were determined to be identical with that of **12** based on detailed comparison of their 1D NMR data and ROESY experiments (see supporting information S88 and S95†).

Chubularisins O (**15**) and P (**16**) were assigned molecular formulae of $\text{C}_{39}\text{H}_{48}\text{O}_{17}$ and $\text{C}_{37}\text{H}_{46}\text{O}_{16}$ by HR-ESI(+)MS based on their pseudo molecular ion peaks at m/z $[\text{M} + \text{Na}]^+$ 811.2808 (calcd 811.2784) and 769.2699 (calcd 769.2678), respectively. The NMR data (Table 5) of compound **15** were highly similar with those of chuktabularin B,^{5a} the exclusive difference being the substitution of the C-12 acetyl in chuktabularin B by an isobutyryl group in **15** (δ_{H} 1.15, d, $J = 6.9$ Hz, 3H; 1.17 d, $J = 6.8$ Hz, 3H; and 2.56, m; δ_{C} 18.8, 19.0, 34.0, and 175.9), which was further affirmed by the HMBC correlation from H-12 (δ_{H} 5.52, d, $J = 3.5$ Hz) to the isobutyryl carbonyl (δ_{C} 175.9). Compared with **15**, compound **16** exhibited more structural variations as listed below: the replacement of the 2-acetyloxy by a hydroxyl (δ_{H} 3.66, s) and the substitution of the 12-isobutyryloxy by a propionyloxy (δ_{H} 1.11, t, $J = 7.5$, 3H and 2.35, m, 2H; δ_{C} 9.0 and 27.2), as well as the appearance of an ethyl (δ_{H} 1.10, t, $J = 7.5$, 3H and 2.04, m, 2H; δ_{C} 8.2 and 26.1) instead of the methyl at C-31 position. The relative configurations of compounds **15** and **16** were identified to be the same as that of chuktabularin B^{5a} based on careful comparison of 1D NMR data and ROESY experiments (see supporting information S102 and S109†).

Chubularisins Q (**17**) and R (**18**) showed pseudo molecular ion peaks $[\text{M} + \text{Na}]^+$ at m/z 783.2841 and 769.2668 in HR-

ESI(+)MS, correspondent with molecular formulae $\text{C}_{38}\text{H}_{48}\text{O}_{16}$ (calcd 783.2835) and $\text{C}_{37}\text{H}_{46}\text{O}_{16}$ (calcd 769.2678), respectively. The NMR data (Table 5) of compound **17** revealed that it was a close structural congener of **15**, with a 3-hydroxyl (δ_{H} 3.76, d, $J = 5.4$) and a 31-ethyl (δ_{H} 1.06, t, $J = 7.5$, 3H and 1.99, m, 2H; δ_{C} 7.6 and 25.8) rather than the corresponding 3-acetyloxy and 31-methyl in **15**, which was characterized by the upfield shifted H-3 (δ_{H} 3.92, d, $J = 5.4$, $\Delta\delta_{\text{H}}$ 1.43 ppm) signal and the presence of the ethyl resonances. Similarly, compound **18** only differentiated from **15** in the replacements of a 31-isopropyl (δ_{H} 1.09, d, $J = 6.8$, 3H; 1.10, d, $J = 7.0$, 3H, and 2.24, m; δ_{C} 17.0, 17.7 and 31.5), a 12-acetyloxy (δ_{H} 2.06, s, 3H; δ_{C} 20.6 and 170.0), and a 2-hydroxyl (δ_{H} 3.66 s), accordingly. The relative chemistry of compounds **17** and **18** were elucidated to be identical with that of **15** as explained by detailed NMR data particularly ROESY experiments (see supporting information S116 and S123†).

Eleven known compounds were identified to be tabularisin A (**19**),⁶ chukvelutin C (**20**),^{2d} tabularisin C (**21**),⁶ tabulalide F (**22**),¹² tabularisin J (**23**),^{5c} tabularisin L (**24**),^{5c} tabulalide G (**25**),¹² chuktabularin F (**26**),^{2c} chuktabularin G (**27**),^{2c} chukvelutin A (**28**),^{2d} and tabularisin B (**29**)⁶ on the basis of comparison of their NMR and ESIMS data with literature values.

All the compounds except **6** (lack of enough material) were tested on voltage-gated potassium (Kv1.2) channel using whole-cell voltage-clamp recording in Chinese hamster ovary (CHO) cells, and 4-aminopyridine (4-AP) was used as a positive control (IC_{50} 279.7 ± 0.12 μM). Interestingly, at a concentration of 30 μM (Table 6), most of the tested compounds exhibited an inhibitory rate of over 0.50. Additionally, selected compounds **4**, **8**, and **22** showed significant inhibition on Kv1.2 with the IC_{50} of 0.61, 2.03, and 2.15 μM , respectively (Fig. 2).

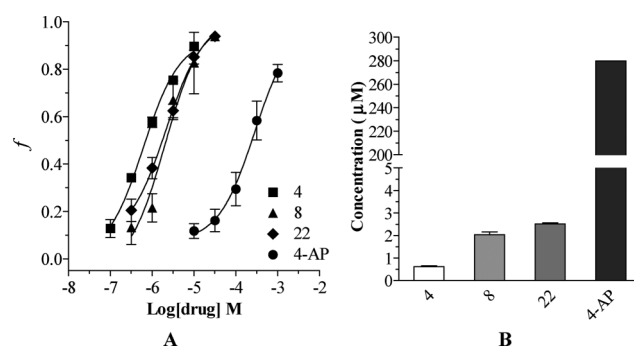


Fig. 2 Inhibition of Kv1.2 channels by compounds **4**, **8**, **22**, and 4-AP. (A) Concentration-response curves of the inhibitory effects of compounds on Kv1.2 channels ($n = 5$); “f” represents normalized current $[(I_{\text{control}} - I_{\text{compound}})/I_{\text{control}}]$; the curves were fitted in a Boltzmann equation. (B) The IC_{50} of each compound on Kv1.2 channels was calculated and presented as histograms (0.61 μM , 2.03 μM , 2.15 μM , and 279.7 μM for compound **4**, **8**, **22**, and 4-AP, respectively).

Conclusions

In summary, this paper describes the isolation and structure elucidation of eighteen new limonoids, chubularisins A–R (**1**–**18**), along with eleven known analogues isolated from the stem bark of *Chukrasia tabularis*. The structure of **1** represented the first example of 8,9,12-orthoester of phragmalin limonoids.

Table 6 Inhibitory effects on Kv1.2 for all the isolates except **6**

Compound No.	Concentration (μM)	Inhibitory Rate
1	30	0.69 ± 0.04
2	30	0.68 ± 0.02
3	30	0.51 ± 0.06
4	30	0.91 ± 0.02
5	30	0.90 ± 0.02
7	30	0.72 ± 0.03
8	30	0.94 ± 0.01
9	30	0.86 ± 0.02
10	30	0.40 ± 0.05
11	30	0.88 ± 0.02
12	30	0.75 ± 0.03
13	30	0.42 ± 0.06
14	30	0.55 ± 0.02
15	30	0.69 ± 0.07
16	30	0.61 ± 0.09
17	30	0.51 ± 0.07
18	30	0.70 ± 0.05
19	30	0.84 ± 0.04
20	30	0.46 ± 0.09
21	30	0.81 ± 0.04
22	30	0.94 ± 0.02
23	30	0.71 ± 0.05
24	30	0.67 ± 0.08
25	30	0.77 ± 0.08
26	30	0.53 ± 0.03
27	30	0.81 ± 0.04
28	30	0.63 ± 0.04
29	30	0.81 ± 0.05

Values are expressed as means \pm SEM for five cells per group.

Compounds **4**, **8**, and **22** exhibited significant activities on the delayed rectifier (I_K) K^+ current with IC_{50} values of 0.61, 2.03, and 2.15 μM , respectively, implicating these compounds could be potential neuroprotective agents.

Experimental section

General experimental procedures

Optical rotations were measured on a Perkin-Elmer 341 polarimeter. UV spectra were measured on a Shimadzu UV-2550 spectrophotometer. IR spectra were recorded on a Perkin-Elmer 577 spectrometer with KBr disks. NMR spectra were measured on a Bruker AM-400 spectrometer with TMS as internal standard. ESIMS and HRESIMS were carried out on a Bruker Daltonics esquire3000plus instrument and a Waters Q-TOF ultima mass spectrometer, respectively. Semipreparative HPLC was performed on a Waters 1525 pump equipped with a Waters 2489 detector and a YMC-Pack ODS-A column (250 \times 10 mm, S-5 μm , 12 nm). All solvents were of analytical grade (Shanghai Chemical Plant, Shanghai, People's Republic of China). Silica gel (200–300 mesh) was used for normal phase column chromatography, and precoated silica gel GF254 plates (Qingdao Haiyang Chemical Plant, Qingdao, People's Republic of China) were used for TLC. C18 reversed-phased silica gel (150–200 mesh, Merck), MCI gel (CHP20P, 75–150 μm , Mitsubishi Chemical Industries Ltd.), D101-macroporous absorption resin (Shanghai Hualing Resin Co., Ltd.), and Sephadex LH-20 gel (Amersham Biosciences) were also used for column chromatography.

Plant material

Chukrasia. tabularis A. Juss. was collected in Hainan Island, People's Republic of China, and was identified by Prof. Shi-Man Huang, Department of Biology, Hainan University, P. R. China.. A voucher specimen has been deposited in Shanghai Institute of Materia Medica, Chinese Academy of Sciences (accession number: STBCT-2006-2Y).

Extraction and isolation

The air-dried stem bark powder (9.0 kg) was percolated with 95% ethanol, and the crude extract (2.0 kg) was subsequently extracted with EtOAc. The EtOAc-soluble fraction (470 g) was separated by D101-macroporous absorption resin CC eluted with a gradient of EtOH/ H_2O (0:100 to 100:0) to give four fractions (A–D). Fraction C (60.0 g) was then separated on a MCI-gel column eluted with CH_3OH/H_2O (0:100 to 100:0, v/v) to give three fractions (C1–C3). Fraction C2 (33.0 g) was applied to a silica-gel column (petroleum ether/ Me_2CO , 20:1 to 0:1) to give nine fractions (C2a–C2i). Fraction C2b (0.70 g) was subjected to CC of silica gel (CH_2Cl_2/CH_3OH , 200:1 to 20:1) to give three fractions (C2b1–C2b3). Fraction C2b1 was purified by a semipreparative HPLC with 60% methanol in water to yield compound tabularisin L (15 mg). Fraction C2b2 was applied to CC of reversed-phase C18 silica gel ($MeOH/H_2O$, 30:70 to 70:30, v/v) and then separated by preparative HPLC (CH_3CN/H_2O , 55:45, 3 ml min^{-1}) to yield **6** (3 mg). Fraction C3c (10.55 g) was subjected to CC of a reversed-phase C18 silica gel ($MeOH/H_2O$, 50:50 to 100:0, v/v) to give two parts (C3c1–C3c2). C3c1 (5.5 g) was separated on a silica gel column eluted with petroleum ether–acetone (5:1 to 0:1) to give two fractions (C3c1A–C3c1B). C3c1A was chromatographed on a silica gel column, eluted with chloroform–methanol (200:1 to 10:1), to give two subfractions, C3c1A1–C3c1A2. Fraction C3c1A1 was then subjected to passage over a column of Sephadex LH-20 gel eluted with EtOH to obtain three subfractions, which were purified by a semipreparative HPLC with 65% acetonitrile in water to yield compound tabularisin B (23 mg) and **11** (11 mg), and tabularisin J (13 mg), respectively. C3c1A2 afforded tabularisin C (60 mg) using semipreparative HPLC (CH_3CN/H_2O , 65:35, 3 ml min^{-1}). Fraction C3c1B was separated on a column of Sephadex LH-20 gel to obtain two subfractions, C3c1B1 and C3c1B2. C3c1B1 was chromatographed on a silica gel column, eluted with petroleum ether/ethyl acetate (4:1 to 1:2), to give **12** (12 mg), **13** (7 mg), **14** (3 mg). Fraction C3c1B2 was subjected to CC of silica gel (petroleum ether/acetone, 4:1 to 0:1) to give four parts (C3c1B2A–C3c1B2D). C3c1B2B was purified by a semipreparative HPLC (CH_3CN/H_2O , 60:40 3 ml min^{-1}) to yield chukvelutin A (12 mg), **4** (3 mg) and **18** (13 mg). By using the same purification procedures, fractions C3c1B2C yielded **5** (16 mg), **15** (5 mg), **16** (11 mg), **17** (10 mg), chukvelutin C (23 mg), and chuktabularin F (19 mg) and fraction C3c1B2D afforded chuktabularin G (58 mg). Fraction C3c2 (3.9 g) was then subjected to passage over a column of a reversed-phase C18 gel eluted with $MeOH/H_2O$ (50:50 to 90:10) to obtain two subfractions, C3c2A and C3c2B. C3c2A (1315 mg) was separated on a column of Sephadex LH-20 gel to obtain three parts (C3c2A1–C3c2A3). C3c2A1 (35 mg) was further separated by semi-preparative HPLC with 70% acetonitrile in water as the mobile phase, to yield

tabularide F (13 mg) and **2** (8 mg). Following the same purification procedures, fraction C3c2A2 gave **7** (7 mg) and **10** (8 mg); fraction C3c2A3 yielded **8** (4 mg) and **9** (9 mg). C3c2B (0.90 g) was subjected to CC of a silica gel ($\text{CH}_2\text{Cl}_2/\text{CH}_3\text{OH}$, 100 : 1 to 10 : 1) to give three parts (C3c2B1–C3c2B2). C3c2B1 was purified by a reversed-phase C18 silica-gel column ($\text{CH}_3\text{OH}/\text{H}_2\text{O}$, 60 : 40 3 ml min^{-1}) to yield tabularisin A (76 mg). Fraction C3c2B2 (150 mg) was subjected to semi-preparative HPLC ($\text{CH}_3\text{OH}/\text{H}_2\text{O}$, 70 : 30 to 100 : 0, 3 ml min^{-1}) to afford tabularide G (12 mg) and **3** (8 mg). C3c2B3 (50 mg) was separated by semipreparative HPLC ($\text{CH}_3\text{CN}/\text{H}_2\text{O}$, 50 : 50, 4 ml min^{-1}) to give **1** (7 mg).

Chubularisin A (1): white amorphous powder; $[\alpha]_{\text{D}}^{20} +77.0$ (*c* 0.500, CHCl_3); UV (MeOH) λ_{max} (log ϵ) 215 (3.56) nm; IR (KBr) ν_{max} 3440, 2980, 1740, 1464, 1402, 1351, 1295, 1219, 1170, 1122, 1075, 1053, 922 cm^{-1} ; ^1H and ^{13}C NMR data, see Table 1 and Table 3; LR-ESI(+)MS m/z 703.3 $[\text{M} + \text{H}]^+$, 725.2 $[\text{M} + \text{Na}]^+$, 1427.5 $[2\text{M} + \text{Na}]^+$; HR-ESI(+)MS m/z 725.2426 $[\text{M} + \text{Na}]^+$ (calcd for $\text{C}_{35}\text{H}_{42}\text{NaO}_{15}$, 725.2416).

Chubularisin B (2): white amorphous powder; $[\alpha]_{\text{D}}^{20} +58.0$ (*c* 0.250, CHCl_3); UV (MeOH) λ_{max} (log ϵ) 215 (3.53) nm; IR (KBr) ν_{max} 3527, 2976, 1728, 1462, 1439, 1369, 1315, 1236, 1162, 1028, 908 cm^{-1} ; ^1H and ^{13}C NMR data, see Table 1 and Table 3; LR-ESI(+)MS m/z 725.2 $[\text{M} + \text{Na}]^+$, 1427.4 $[2\text{M} + \text{Na}]^+$; HR-ESI(+)MS m/z 725.2415 $[\text{M} + \text{Na}]^+$ (calcd for $\text{C}_{35}\text{H}_{42}\text{NaO}_{15}$, 725.2416).

Chubularisin C (3): white amorphous powder; $[\alpha]_{\text{D}}^{20} +36.0$ (*c* 0.090, CHCl_3); UV (MeOH) λ_{max} (log ϵ) 206 (3.13) nm; IR (KBr) ν_{max} 3439, 2978, 1749, 1470, 1439, 1371, 1242, 1159, 1088, 1020, 986, 903 cm^{-1} ; ^1H and ^{13}C NMR data, see Table 1 and Table 3; LR-ESI(+)MS m/z 797.2 $[\text{M} + \text{Na}]^+$, 1571.4 $[2\text{M} + \text{Na}]^+$; HR-ESI(+)MS m/z 797.2609 $[\text{M} + \text{Na}]^+$ (calcd for $\text{C}_{38}\text{H}_{46}\text{NaO}_{17}$, 797.2627).

Chubularisin D (4): white amorphous powder; $[\alpha]_{\text{D}}^{20} +10.4$ (*c* 0.800, CHCl_3); UV (MeOH) λ_{max} (log ϵ) 206 (3.13) nm; IR (KBr) ν_{max} 3543, 2978, 1767, 1740, 1464, 1427, 1375, 1362, 1327, 1290, 1244, 1203, 1078, 1036, 986, 893 cm^{-1} ; ^1H and ^{13}C NMR data, see Table 1 and Table 3; LR-ESI(+)MS m/z 839.3 $[\text{M} + \text{Na}]^+$, 1655.3 $[2\text{M} + \text{Na}]^+$; HR-ESI(+)MS m/z 839.2731 $[\text{M} + \text{Na}]^+$ (calcd for $\text{C}_{40}\text{H}_{48}\text{NaO}_{18}$, 839.2733).

Chubularisin E (5): white amorphous powder; $[\alpha]_{\text{D}}^{20} +45.0$ (*c* 0.150, CHCl_3); UV (MeOH) λ_{max} (log ϵ) 205 (3.56) nm; IR (KBr) ν_{max} 3514, 2976, 1759, 1736, 1470, 1427, 1375, 1325, 1290, 1242, 1200, 1151, 1119, 1034, 1001, 889 cm^{-1} ; ^1H and ^{13}C NMR data, see Table 1 and Table 3; LR-ESI(+)MS m/z 853.3 $[\text{M} + \text{Na}]^+$, 1683.4 $[2\text{M} + \text{Na}]^+$; HR-ESI(+)MS m/z 853.2888 $[\text{M} + \text{Na}]^+$ (calcd for $\text{C}_{41}\text{H}_{50}\text{NaO}_{18}$, 853.2889).

Chubularisin F (6): white amorphous powder; $[\alpha]_{\text{D}}^{20} +33.0$ (*c* 0.015, CHCl_3); UV (MeOH) λ_{max} (log ϵ) 206 (3.33) nm; IR (KBr) ν_{max} 3435, 2922, 1749, 1635, 1390, 1232, 1051 cm^{-1} ; ^1H and ^{13}C NMR data, see Table 2 and Table 3; LR-ESI(+)MS m/z 777.3 $[\text{M} + \text{H}]^+$, 799.3 $[\text{M} + \text{Na}]^+$; HR-ESI(+)MS m/z 799.2434 $[\text{M} + \text{Na}]^+$ (calcd for $\text{C}_{37}\text{H}_{44}\text{NaO}_{18}$, 799.2420).

Chubularisin G (7): white amorphous powder; $[\alpha]_{\text{D}}^{20} +29.0$ (*c* 0.240, CHCl_3); UV (MeOH) λ_{max} (log ϵ) 206 (3.30) nm; IR (KBr) ν_{max} 3437, 2978, 1755, 1730, 1371, 1215, 1097, 1024, 912 cm^{-1} ; ^1H and ^{13}C NMR data, see Table 2 and Table 3; LR-ESI(+)MS m/z 883.2 $[\text{M} + \text{Na}]^+$; HR-ESI(+)MS m/z 883.2641 $[\text{M} + \text{Na}]^+$ (calcd for $\text{C}_{41}\text{H}_{48}\text{NaO}_{20}$, 883.2631).

Chubularisin H (8): white amorphous powder; $[\alpha]_{\text{D}}^{20} +17.2$ (*c* 0.500, CHCl_3); UV (MeOH) λ_{max} (log ϵ) 205 (3.36) nm; IR (KBr) ν_{max} 3541, 3496, 2980, 1751, 1470, 1405, 1371, 1288, 1221, 1134, 1024, 891 cm^{-1} ; ^1H and ^{13}C NMR data, see Table 2 and Table 3; LR-ESI(+)MS m/z 911.3 $[\text{M} + \text{Na}]^+$; HR-ESI(+)MS m/z 911.2960 $[\text{M} + \text{Na}]^+$ (calcd for $\text{C}_{43}\text{H}_{52}\text{NaO}_{20}$, 911.2944).

Chubularisin I (9): white amorphous powder; $[\alpha]_{\text{D}}^{20} +4.0$ (*c* 0.100, CHCl_3); UV (MeOH) λ_{max} (log ϵ) 206 (3.36) nm; IR (KBr) ν_{max} 3435, 2978, 2928, 1759, 1734, 1635, 1421, 1363, 1229, 1134, 1024, 891 cm^{-1} ; ^1H and ^{13}C NMR data, see Table 2 and Table 3; LR-ESI(+)MS m/z 839.3 $[\text{M} + \text{Na}]^+$; HR-ESI(+)MS m/z 839.2753 $[\text{M} + \text{Na}]^+$ (calcd for $\text{C}_{40}\text{H}_{48}\text{NaO}_{18}$, 839.2733).

Chubularisin J (10): white amorphous powder; $[\alpha]_{\text{D}}^{20} -100.0$ (*c* 0.030, CHCl_3); UV (MeOH) λ_{max} (log ϵ) 206 (3.36) nm; IR (KBr) ν_{max} 3435, 2924, 1753, 1373, 1219, 1097, 1059, 1031, 902 cm^{-1} ; ^1H and ^{13}C NMR data, see Table 2 and Table 3; LR-ESI(+)MS m/z 925.2 $[\text{M} + \text{Na}]^+$; HR-ESI(+)MS m/z 925.2742 $[\text{M} + \text{Na}]^+$ (calcd for $\text{C}_{43}\text{H}_{50}\text{NaO}_{21}$, 925.2737).

Chubularisin K (11): white amorphous powder; $[\alpha]_{\text{D}}^{20} -99.1$ (*c* 0.330, CHCl_3); UV (MeOH) λ_{max} (log ϵ) 206 (3.37) nm; IR (KBr) ν_{max} 3547, 3489, 3016, 2978, 1759, 1468, 1421, 1371, 1288, 1221, 1136, 1024, 891 cm^{-1} ; ^1H and ^{13}C NMR data, see Table 2 and Table 3; LR-ESI(+)MS m/z 861.2 $[\text{M} + \text{H}]^+$, 883.2 $[\text{M} + \text{Na}]^+$; HR-ESI(+)MS m/z 883.2640 $[\text{M} + \text{Na}]^+$ (calcd for $\text{C}_{41}\text{H}_{48}\text{NaO}_{20}$, 883.2631).

Chubularisin L (12): white amorphous powder; $[\alpha]_{\text{D}}^{20} -25$ (*c* 0.260, CHCl_3); UV (MeOH) λ_{max} (log ϵ) 207 (3.37), 268 (3.33) nm; IR (KBr) ν_{max} 3448, 2974, 1740, 1470, 1369, 1300, 1230, 1161, 1062, 1028, 993 cm^{-1} ; ^1H and ^{13}C NMR data, see Table 4; LR-ESI(+)MS m/z 921.4 $[\text{M} + \text{Na}]^+$; HR-ESI(+)MS m/z 921.3516 $[\text{M} + \text{Na}]^+$ (calcd for $\text{C}_{46}\text{H}_{58}\text{NaO}_{18}$, 921.3515).

Chubularisin M (13): white amorphous powder; $[\alpha]_{\text{D}}^{20} -6$ (*c* 0.125, CHCl_3); UV (MeOH) λ_{max} (log ϵ) 208 (3.31), 268 (3.25) nm; IR (KBr) ν_{max} 3435, 2976, 2937, 1761, 1745, 1655, 1599, 1470, 1402, 1267, 1219, 1142, 1061, 1024, 993 cm^{-1} ; ^1H and ^{13}C NMR data, see Table 4; LR-ESI(+)MS m/z 963.4 $[\text{M} + \text{Na}]^+$; HR-ESI(+)MS m/z 963.3641 $[\text{M} + \text{Na}]^+$ (calcd for $\text{C}_{48}\text{H}_{60}\text{NaO}_{19}$, 963.3621).

Chubularisin N (14): white amorphous powder; $[\alpha]_{\text{D}}^{20} -3$ (*c* 0.100, CHCl_3); UV (MeOH) λ_{max} (log ϵ) 207 (3.31), 268 (3.25) nm; IR (KBr) ν_{max} 3440, 2976, 2937, 1747, 1647, 1605, 1470, 1387, 1219, 1144, 1061, 997, 901 cm^{-1} ; ^1H and ^{13}C NMR data, see Table 4; LR-ESI(+)MS m/z 949.4 $[\text{M} + \text{Na}]^+$; HR-ESI(+)MS m/z 949.3466 $[\text{M} + \text{Na}]^+$ (calcd for $\text{C}_{47}\text{H}_{58}\text{NaO}_{19}$, 949.3465).

Chubularisin O (15): white amorphous powder; $[\alpha]_{\text{D}}^{20} +33$ (*c* 0.150, CHCl_3); UV (MeOH) λ_{max} (log ϵ) 206 (3.31) nm; IR (KBr) ν_{max} 3581, 3431, 2982, 2941, 1751, 1462, 1373, 1298, 1244, 1221, 1149, 1126, 1095, 1040, 924 cm^{-1} ; ^1H and ^{13}C NMR data, see Table 5; LR-ESI(+)MS m/z 811.3 $[\text{M} + \text{Na}]^+$; HR-ESI(+)MS m/z 811.2808 $[\text{M} + \text{Na}]^+$ (calcd for $\text{C}_{39}\text{H}_{48}\text{NaO}_{17}$, 811.2784).

Chubularisin P (16): white amorphous powder; $[\alpha]_{\text{D}}^{20} +210$ (*c* 0.010, CHCl_3); UV (MeOH) λ_{max} (log ϵ) 206 (3.77) nm; IR (KBr) ν_{max} 3437, 2980, 1751, 1462, 1375, 1296, 1221, 1149, 1088, 1032, 976 cm^{-1} ; ^1H and ^{13}C NMR data, see Table 5; LR-ESI(+)MS m/z 769.3 $[\text{M} + \text{Na}]^+$; HR-ESI(+)MS m/z 769.2699 $[\text{M} + \text{Na}]^+$ (calcd for $\text{C}_{37}\text{H}_{46}\text{NaO}_{16}$, 769.2678).

Chubularisin Q (17): white amorphous powder; $[\alpha]_{\text{D}}^{20} +68$ (*c* 0.025, CHCl_3); UV (MeOH) λ_{max} (log ϵ) 206 (3.46) nm; IR (KBr)

ν_{\max} 3437, 2976, 2931, 1749, 1371, 1254, 1223, 1148, 1124, 1041, 922 cm^{-1} ; ^1H and ^{13}C NMR data, see Table 5; LR-ESI(+)MS m/z 783.3 $[\text{M} + \text{Na}]^+$; HR-ESI(+)MS m/z 783.2841 $[\text{M} + \text{Na}]^+$ (calcd for $\text{C}_{38}\text{H}_{48}\text{NaO}_{16}$, 783.2835).

Chubularisin R (18): white amorphous powder; $[\alpha]_{\text{D}}^{20} +38$ (c 0.100, CHCl_3); UV (MeOH) λ_{\max} ($\log \epsilon$) 206 (3.31) nm; IR (KBr) ν_{\max} 3437, 2976, 1751, 1373, 1296, 1227, 1149, 1092, 1034, 980 cm^{-1} ; ^1H and ^{13}C NMR data, see Table 5; LR-ESI(+)MS m/z 769.3 $[\text{M} + \text{Na}]^+$; HR-ESI(+)MS m/z 769.2668 $[\text{M} + \text{Na}]^+$ (calcd for $\text{C}_{37}\text{H}_{46}\text{NaO}_{16}$, 769.2678).

Kv1.2 Assay

Chinese hamster ovary (CHO) cells were plated into 6-well dish and transfected with the Kv1.2 expression plasmid. One day after the transfection, CHO cells were seeded into glass-plate, and the whole-cell voltage-clamp recording was performed in these cells 15 h later.

Statistical Analysis

Data are presented as means \pm standard error of the mean (SEM) of measurements made on 5 cells in each group.

Acknowledgements

Financial support of the National Natural Science Foundation (Grant No. 81021062; 20902095), and National Science & Technology Major Project "Key New Drug Creation and Manufacturing Program" (Number: 2011ZX09307-002-03) of the People's Republic of China are gratefully acknowledged. We thank Prof. S.-M. Huang of Hainan University for the identification of the plant material.

References

- (a) A. Roy and S. Saraf, *Biol. Pharm. Bull.*, 2006, **29**, 191–201; (b) D. A. Mulholland, B. Parel and P. H. Coombes, *Curr. Org. Chem.*, 2000, **4**, 1011–1054; (c) D. E. Champagne, O. Koul, M. B. Isman, G. G. E. Scudder and G. H. N. Towers, *Phytochemistry*, 1992, **31**, 377–394; (d) A. Akhila and K. Rani, in *Progress in the Chemistry of Organic Natural Products*, ed. W. Herz, H. Falk, G. W. Kirby and R. E. Moore, Springer, Vienna, 1999, vol. 78, pp 47–149.
- (a) J. D. Connolly, C. Labbé and D. S. Rycroft, *J. Chem. Soc., Perkin Trans. 1*, 1978, 285–288; (b) T. Ragettli and C. Tamm, *Helv. Chim. Acta*, 1978, **61**, 1814–1831; (c) J. Luo, J.-S. Wang, X.-B. Wang, J.-G. Luo and L.-Y. Kong, *J. Nat. Prod.*, 2010, **73**, 835–843; (d) J. Luo, J.-S. Wang, J.-G. Luo, X.-B. Wang and L.-Y. Kong, *Org. Lett.*, 2009, **11**, 2281–2284; (e) M. Nakatani, S. A. M. Abdelgaleil, M. M. G. Saad, R. C. Huang, M. Doe and T. Iwagawa, *Phytochemistry*, 2004, **65**, 2833–2841.
- S. K. Chen, B. Y. Chen and H. Li, in *Flora Republicae Popularis Sinicae (Zhongguo Zhiwu Zhi)*, Science Press, Beijing, 1997, Vol. 43(3), pp 47–49.
- Chinese Materia Medica (Zhonghua Bencao)*, Editorial Committee of the Administration Bureau of Traditional Chinese Medicine; Shanghai Science and Technology Press, Shanghai, 1999, Vol. 5, pp 31–32.
- (a) C.-R. Zhang, S.-P. Yang, S.-G. Liao, C.-Q. Fan, Y. Wu and J.-M. Yue, *Org. Lett.*, 2007, **9**, 3383–3386; (b) C.-R. Zhang, C.-Q. Fan, L. Zhang, S.-P. Yang, Y. Wu, Y. Lu and J.-M. Yue, *Org. Lett.*, 2008, **10**, 3183–3186; (c) C.-R. Zhang, S.-P. Yang, X.-Q. Chen, Y. Wu, X.-C. Zhen and J.-M. Yue, *Helv. Chim. Acta*, 2008, **91**, 2338–2350.
- C.-Q. Fan, X.-N. Wang, S. Yin, C.-R. Zhang, F.-D. Wang and J.-M. Yue, *Tetrahedron*, 2007, **63**, 6741–6747.
- C.-C. Shieh, M. Coghlan, J. P. Sullivan and M. Gopalakrishnan, *Pharmacol. Rev.*, 2000, **52**, 557–593.
- H. Liu, Y. Li, M. K. Song, X. J. Tan, F. Cheng, S. X. Zheng, J. H. Shen, X. M. Luo, R. Y. Ji, J. M. Yue, G. Y. Hu, H. L. Jiang and K. X. Chen, *Chem. Biol.*, 2003, **10**, 1103–1113.
- C.-R. Zhang, S.-P. Yang, Q. Zhu, S.-G. Liao, Y. Wu and J.-M. Yue, *J. Nat. Prod.*, 2007, **70**, 1616–1619.
- S.-G. Liao, H.-D. Chen and J.-M. Yue, *Chem. Rev.*, 2009, **109**, 1092–1140.
- J. Luo, J.-S. Wang, X.-B. Wang, X.-F. Huang, J.-G. Luo and L.-Y. Kong, *Tetrahedron*, 2009, **65**, 3425–3431.
- J. Luo, J.-S. Wang, X.-B. Wang, J.-G. Luo and L.-Y. Kong, *Chem. Pharm. Bull.*, 2011, **59**, 225–230.